NMR Relaxation and Neutron Scattering in a Fermi-Liquid Picture of the Metallic Copper Oxides

Jian Ping Lu, Qimiao Si, Ju H. Kim, and K. Levin
Department of Physics and the James Franck Institute and Science and Technology Center for Superconductivity, The University of Chicago, Chicago, Illinois 60637
(Received 12 February 1990)

Using a Fermi-liquid formalism in which the Cu d electrons are quasilocalized, we calculate the NMR relaxation for the Cu and O sites, the temperature-dependent magnetic susceptibility, and the neutron-scattering cross section. Our microscopic calculations of the dynamical susceptibility help to decouple narrow-band phenomena from spin-fluctuation effects. The former lead to a low (coherence) energy scale and considerable structure in the Lindhard function. The latter help to enhance these effects.

PACS numbers: 74.70.Vy, 75.20.Hr, 76.60.Es

In this paper we investigate a variety of magnetic data[1-4] in the metallic copper oxides using a microscopically based Fermi-liquid approach in which the $3d$ electrons are almost localized. This scheme incorporates the strong Coulomb correlations, necessary to explain the Mott-insulating state at half filling, and has been applied elsewhere to discuss transport properties.[5] Previous Fermi-liquid-like[6,7] schemes have explained the low characteristic energy scale (~ 150 K) seen in $1/T_1$ for Cu and the difference between Cu and O relaxation rates by assuming that the copper oxides are nearly antiferromagnetic. On the basis of experimental evidence in the metallic state which suggests[8,9] that the Cu valence is near $+2$ and the magnetic moment nearly integral,[1,9] we argue that the d electrons are "almost localized." This leads to a moderately heavy mass. This incipient localization is associated with a low energy scale which we call the "coherence" energy $T_{\rm coh}$, and which represents some fraction of the degeneracy temperature of the d electrons.[10] The present analysis suggests that there is a delicate interplay between this narrow-band effect and spin fluctuations which may also lead to low energy scales.[6,7] While we cannot rule out this scenario, we show that to obtain reasonable agreement with magnetic data, it may not be necessary to assume these systems are right at the verge of a magnetic instability.

Our starting point is the standard, large-U, CuO_2 tight-binding Hubbard Hamiltonian. (For definiteness, we work in the "electron" picture. Equivalent results for the "hole" picture are presented elsewhere.[11]) We chose the parameters such that, in the standard notation,[5] $\varepsilon_p - \varepsilon_d^0 = 4$ eV, $t_{pd} = 1.6$ eV, and $t_{pp} = 0.4$ eV. At the mean-field level,[5] the effect of large or essentially infinite U is to introduce a constraint into the Hamiltonian that there be no double occupancy. In this way the Cu-O hybridization t_{pd} is greatly reduced and the d level ε_d^0 is self-consistently renormalized so as to avoid double occupancy. This procedure is rigorous[5] in the context of a $1/N$ expansion (where N is the spin degeneracy of the electrons). With the incorporation of these two renormalizations, the Hamiltonian reduces to an effective noninteracting extended Hubbard Hamiltonian. A diagonalization (made somewhat more complex by the presence of oxygen-oxygen overlap t_{pp}) then produces a renormalized band structure $E_n(k)$ which characterizes the quasiparticles of the Fermi liquid. These are composed of hybridized copper and oxygen states with corresponding coherence factors $u_{nr}(k)$ (where the index $n = 1,2,3$ refers to one of the three renormalized bands and $r = d, p_x, p_y$ represents Cu or O sites).

Because of these strong Coulomb correlation effects, the renormalized antibonding band is greatly reduced in width. This reduction is hole-concentration dependent and scales[5] with the self-consistently determined d-electron concentration n_d as $t_{pd} \to t_{pd}(1-n_d)^{1/2}$. Thus, as the insulator is approached the band becomes progressively more narrow, reflecting Mott localization.[5] A measure of this band narrowing is the coherence temperature $T_{\rm coh}$, which is roughly $\frac{1}{5}$ of the separation in energy between the Fermi energy and the nearest band edge. This is of the order of several hundred K for a reasonable range of doping concentrations.

The residual quasiparticle exchange interactions J_H may be calculated within this scheme following the work of Houghton, Read, and Won.[9] Formally, this interaction is of order $(1/N)^2$. Within the RPA scheme the dynamical spin susceptibility may then be resummed[9,12] to yield

$$\chi_{rr'}(\mathbf{q},\omega) = \chi^0_{rr'}(\mathbf{q},\omega) + \frac{\chi^0_{rd}(\mathbf{q},\omega)[-J_H(\mathbf{q})]\chi^0_{dr'}(\mathbf{q},\omega)}{1 + J_H(\mathbf{q})\chi^0_{dd}(\mathbf{q},\omega)} . \tag{1a}$$

The Lindhard susceptibility components are

$$\chi^0_{rr'}(\mathbf{q},\omega) = \frac{1}{N}\sum_{nm\mathbf{k}} \frac{f(E_m(\mathbf{k}+\mathbf{q})) - f(E_n(\mathbf{k}))}{\omega - [E_m(\mathbf{k}+\mathbf{q}) - E_n(\mathbf{k})]} u^*_{mr}(\mathbf{k}+\mathbf{q}) u^*_{nr'}(\mathbf{k}) u_{mr'}(\mathbf{k}+\mathbf{q}) u_{nr}(\mathbf{k}) . \tag{1b}$$

While Eq. (1a) formally resembles the approach of Ref. 7, here we have microscopically derived the renormalized parameters χ^0 and $J_H(q)$ appearing in the RPA susceptibility.

This spin-spin exchange interaction $J_H(q)$ includes both superexchange and Ruderman-Kittel-Kasuya-Yosida (RKKY) contributions and is strongly doping-concentration dependent.[9] Like the Lindhard function, it also depends on the self-consistently determined renormalized band structure $E_n(k)$ of the tight-binding Hamiltonian. In the inset of Fig. 1 is plotted the net exchange interaction as a function of wave vector $\mathbf{q}$ for a doping concentration $x=4\%$, where the interaction is dominated by the antiferromagnetic superexchange. Here the insulating limit (100 meV) is fitted. At larger x, the RKKY term dominates and is initially ferromagnetic and ultimately antiferromagnetic as the doping is increased. The overall sign of this exchange interaction for moderate x is parameter and model sensitive and thus cannot be stated with certainty. However, the calculated $\mathbf{q}$ dependence of $J_H(\mathbf{q})$ for metallic concentrations can be approximated by a nearest-neighbor exchange with amplitude J_0. In what follows, we will assume J_0 is of antiferromagnetic sign and its magnitude is chosen to reflect our previous microscopic calculations of the net superexchange plus (ferromagnetic) RKKY interaction. We will also consider values of J_0 which are closer to the instability value J_c. In these units we find microscopically that J_0/J_c is 0.5 and 0.05 for small and large x, respectively. In line with the weak T and ω dependence of the oxygen susceptibility (which mediates the Cu-Cu exchange), we find J_H is essentially independent of these two parameters.

The NMR relaxation rate and corresponding Knight shift are given by

$$\left(\frac{1}{T_1}\right)_r^{\alpha}=\frac{T}{2N}\sum_{\beta}{}'\sum_{r'r''}\sum_{\mathbf{q}}A_{rr'}^{\beta}(\mathbf{q})A_{rr''}^{\beta}(\mathbf{q})\frac{\mathrm{Im}\chi_{r'r''}(\mathbf{q},\omega_0)}{\omega_0}, \tag{2}$$

$$K_r^{\alpha}=\frac{\gamma_e}{2\gamma_N}\sum_{r'r''}A_{rr'}^{\alpha}(\mathbf{q}=0)\chi_{r'r''}(\mathbf{q}\to 0,\omega=0), \tag{3}$$

where ω_0 is the nuclear-magnetic-resonance frequency which is taken to be zero. Here α and β label principle axes. The prime on the summation in Eq. (2) is over principle axes perpendicular to the field orientation α. The physical origin and the $\mathbf{q}$ dependence of the coupling constants A_{dd}, A_{pp}, and A_{pd} is discussed in Ref. 3. (For notational simplicity when $r,r'=p_{x,y}$ we will abbreviate this as p.) We take the q dependence of the hyperfine form factors $A(q)$ as summarized in Ref. 7.

In the following four figures, we plot as open triangles ($x=0.09$) and circles ($x=0.28$) the contributions to various magnetic phenomena which derive solely from χ^0. All results with nonzero J_0 are plotted as solid symbols. At $x=0.28$, for the values of J_0 which we estimate from our microscopic calculations, our results are not substantially different from those shown with $J_0=0$, so that for simplicity we do not plot them here. However, at this higher concentration two larger values of J_0 are indicated by the squares and diamonds. On the basis of simple stoichiometry arguments, this higher concentration may be associated with fully oxygenated Y-Ba-Cu-O. To emphasize only the T and x dependence, the $1/T_1$ and χ curves are normalized so that at $x=0.09$, $T=30$ meV, and $J_0=0$, the corresponding values are unity.

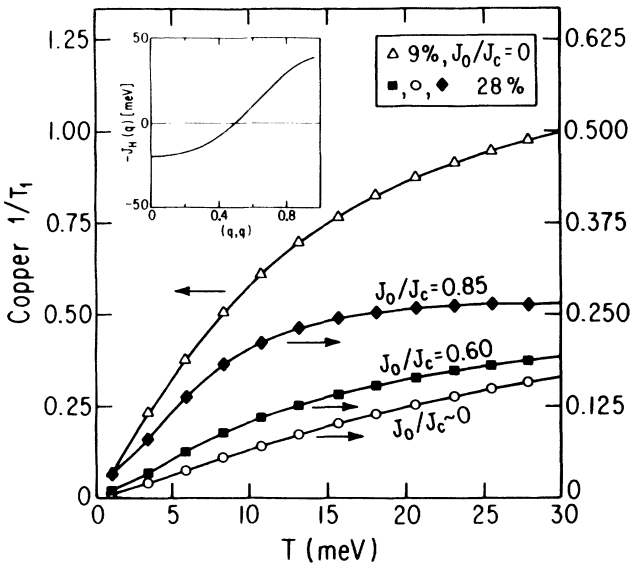

FIG. 1. Normalized (see text) temperature dependence of Cu $1/T_1$ for two hole concentrations x and for various values of the antiferromagnetic exchange. Inset: The full $\mathbf{q}$ dependence at $x=0.04$ of the exchange $J_H(\mathbf{q})$ which has amplitude parametrized by J_0.

In Fig. 1 is plotted the NMR relaxation rate $1/T_1$ as a function of temperature at the Cu sites, assuming[3,6,7] relaxation comes solely from A_{dd}. The behavior of $1/T_1$ is Korringa-like at the lowest temperatures and begins to deviate as T_{coh} is approached. This deviation occurs at higher temperatures, as the concentration is increased. On the other hand, the deviation temperature can be "tuned" by increasing J_0 towards the instability value J_c. Experimentally, similar deviations from Korringa behavior have been reported[2,3] and it has been noted that in the La-Cu-O family, these become less apparent with increased doping.[2] On the basis of these calculations, it follows that spin-spin interactions are not necessary in order to obtain a low characteristic energy scale, nor to fit the T dependence of the Cu NMR relaxation. However, the *effective* on-site Korringa ratio $1/T_1TK^2$ in Y-Ba-Cu-O has been estimated[3] to be around 10. This large value is consistent with the $x=0.28$ curves when J_0 assumes the intermediate value shown by the squares.

In Fig. 2 are plotted the analogous oxygen relaxation rates $1/T_1$ versus temperature for the larger concentration only, corresponding to $YBa_2Cu_3O_7$. The results for the case of relaxation via A_{pp} are shown as dashed lines, whereas the transfer-hyperfine-induced relaxation (via A_{pd}) is shown by the solid curves. In the first case, the T dependence is considerably more Korringa-like than that of the Cu. This difference can be attributed to the fact

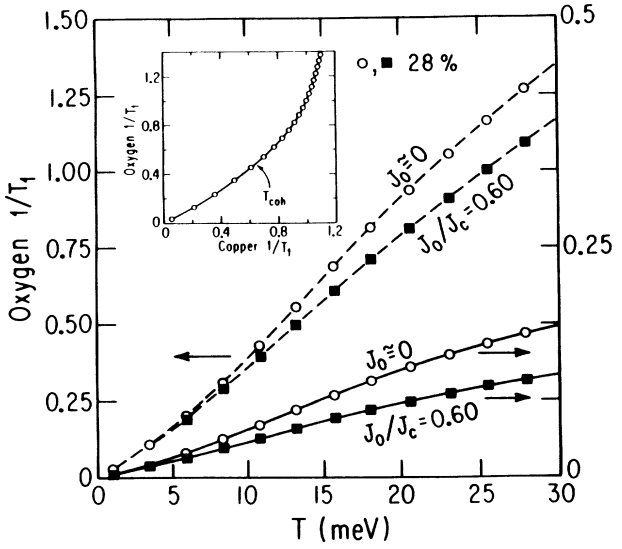

FIG. 2. Temperature dependence of normalized O $1/T_1$ at $x=0.28$, corresponding roughly to $YBa_2Cu_3O_7$ with various values of antiferromagnetic coupling strength. The dashed lines correspond to oxygen-oxygen- and the solid lines to Cu-oxygen-induced relaxation. Inset: The two relaxations as described in text, O $1/T_1$ vs Cu $1/T_1$ for $x=0.09$. The arrow indicates T_{coh}.

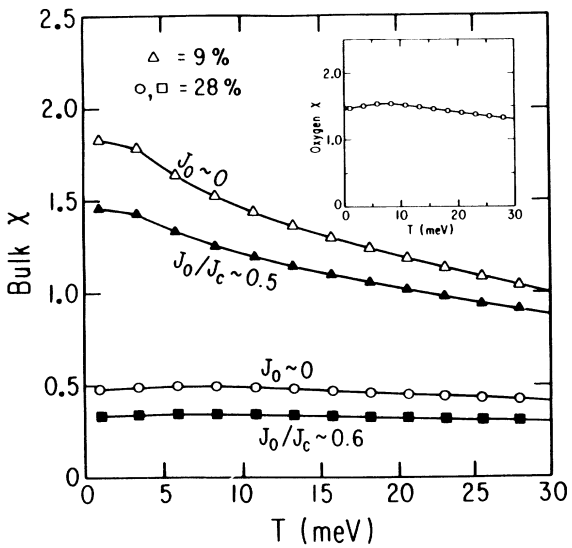

FIG. 3. Temperature dependence of normalized static susceptibility. Inset: The oxygen contribution to χ.

that the coherence temperature T_{coh} is not as apparent in the oxygen band-energy scales since the oxygen states are more uniformly spread out (in energy) throughout the band. The transfer-hyperfine case shows a slight deviation from Korringa behavior due to an imperfect cancellation of the oxygen form-factor contribution, as has also been noticed previously.[7] This deviation becomes more apparent as the hole concentration decreases. Because our curves are normalized to the $x=0.09$ results, it can be seen that the transfer-hyperfine-induced relaxation leads to a *decrease* in the oxygen $1/T_1$ with increasing x, whereas the oxygen-oxygen-induced relaxation leads to the opposite result. The transfer-hyperfine case seems, thus far, to be *inconsistent* with the trends observed in comparing 60- and 90-K samples.[13]

The coherence temperature T_{coh} can be illustrated graphically by plotting the relaxation rate $1/T_1$ for oxygen (deriving from χ^0_{pp}) versus $1/T_1$ for Cu (arising from χ^0_{dd}) as shown in the inset of Fig. 2 for the lower concentration. Although there are a number of different components of the χ matrix, the inset indicates that at low temperatures all contributions "track" in the one-component fashion. They thus do *not* represent independent degrees of freedom. This tracking starts to break down above T_{coh}, where the Cu d states begin to localize and the Fermi liquid loses is coherence.[10] Even in this regime, however, the contributions are highly coupled so that a "two-component" description is inappropriate. By contrast, we find there is always more tracking between the oxygen and Cu Knight shifts than is found in the corresponding $1/T_1$, as a consequence of the "cross term" χ_{pd} (independent of the details of hyperfine coupling). The deviation from a straight line in the inset, indicated by the arrow, identifies T_{coh}. This temperature increases with increased doping concentration such that $T_{coh} \sim 10$ meV for $x=0.09$ and ~ 20 meV for $x=0.28$.

In Fig. 3 is plotted the temperature dependence of the uniform static susceptibility for some of the cases discussed before. The inset corresponds to the oxygen contribution to χ, or Knight shift, at $x=0.28$. The bulk susceptibility which is dominated by the contribution from the Cu states is essentially the Cu Knight shift. At the larger x, χ is relatively flat as seen experimentally for optimal concentrations. At lower x, we find that χ decreases with increasing T. While this behavior is seen in samples near the insulating limit, we do not find the decrease in χ with decreasing T which is reported[2] in slightly deoxygenated samples of Y-Ba-Cu-O.

Finally, in Fig. 4 is plotted the neutron structure factor $S(\mathbf{q},\omega)$ for $x=0.09$ as a function of momentum transfer $\mathbf{q}$ in the (1,1) direction. Here the temperature is taken to be $T=1$ meV and the frequency $\omega=10$ meV. The figure indicates an incommensurate peak at $\mathbf{Q}$ which is near the zone edge at (π,π). This is related to a Kohn anomaly and associated with two dimensionality rather than band structure. The smaller the doping concentration, the more pronounced the peak structure. When peaks are observed at larger x, they are further displaced from the zone edge. As the temperature is raised towards T_{coh} the peak is smeared out. The frequency dependence of the $\mathbf{q}=\mathbf{Q}$ peak height is shown by the inset. Similar peaks have been reported in both the La-Cu-O and Y-Ba-Cu-O families,[4] although in the latter case at reduced oxygen stoichiometries.

In summary, this study has illustrated that (1)

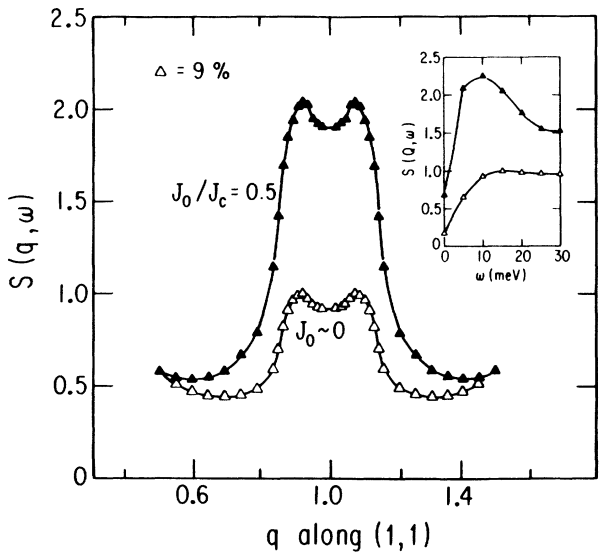

FIG. 4. Structure factor $S(\mathbf{q},\omega)$ vs $\mathbf{q}$. The normalization is chosen so that the value of the lower curve is 1.0 at peak position. Inset: ω dependence of peak height.

narrow-band phenomena lead to low energy scales. These in turn lead to deviations from Korringa behavior for the Cu $1/T_1$, even in the absence of antiferromagnetic interactions. Examples of this narrow-band effect are seen very generally in NMR relaxation of heavy-fermion systems (where T_{coh} is roughly 2 orders of magnitude smaller).[10] (2) There is an important constraint on any Fermi-liquid approach which affects both the Cu and O relaxation. This derives from the $1/q$ dependence of $\mathrm{Im}\chi(q,\omega)/\omega$ as $\omega \to 0$ and $q \to 0$ which heavily weights the small-q regime. Thus very strong antiferromagnetic peaks are required in order to offset this small-q effect and to obtain, for example, an appreciable enhancement of the Korringa ratio on Cu. An additional consequence of this small-q contribution is the delicacy of the Korringa behavior on the O site derived via transfer-hyperfine interactions. This depends on precise cancellations which we and others[7] find to be unstable to small changes in the parameters. We suggest that if future highly accurate experiments find *no* deviations from Korringa behavior for $1/T_1$ at the oxygen sites, one should investigate additional relaxation mechanisms such as orbitally induced processes to explain fully the oxygen Korringa behavior. (3) Based on a variety of data, it is reasonable to assume that both near antiferromagnetism and these narrow-band effects are simultaneously playing a role. By including a combination of these two, it is possible to construct reasonably "robust" models for the metallic copper oxides which are consistent with a variety of different magnetic and transport measurements.

This work was supported by NSF Science and Technology Center Grant No. STC-8809854. We acknowledge receipt of NSF supercomputer funds and helpful conversations with C. Slichter.

[1]For a review of NMR, see C. P. Pennington and C. P. Slichter, in *Physical Properties of High Temperature Superconductors II,* edited by D. M. Ginsberg (World Scientific, Teaneck, NJ, 1990).

[2]See, for example, H. Alloul *et al.*, Phys. Rev. Lett. **63**, 1700 (1989); S. E. Barrett *et al.* (to be published); H. Horvatic *et al.*, Phys. Rev. B **39**, 7332 (1989); T. Imai *et al.* (to be published); M. Takigawa *et al.*, Phys. Rev. B **39**, 7371 (1989); W. W. Warren *et al.*, Phys. Rev. Lett. **62**, 1193 (1989).

[3]P. C. Hammel *et al.*, Phys. Rev. Lett. **63**, 1992 (1989).

[4]G. Shirane *et al.*, Phys. Rev. Lett. **63**, 330 (1989); J. M. Tranquada *et al.* (to be published).

[5]See, J. H. Kim *et al.*, Phys. Rev. B **39**, 1163 (1989); **40**, 11 378 (1989), and references therein.

[6]A. J. Millis, H. Monien, and D. Pines, Phys. Rev. B **42**, 167 (1990).

[7]N. Bulut *et al.*, Phys. Rev. B **41**, 1797 (1990).

[8]J. M. Tranquada, S. M. Heald, A. R. Moodenbaugh, Phys. Rev. B **36**, 5263 (1987), and references therein.

[9]Q. Si, J. P. Lu, and K. Levin, Physica (Amsterdam) **162-164C**, 1467 (1989); see also Q. Si *et al.*, Phys. Rev. B **42**, 1033 (1990); A. Houghton, N. Read, and H. Won, Phys. Rev. B **37**, 3782 (1988).

[10]Qimiao Si *et al.*, Phys. Rev. B **42**, 1033 (1990).

[11]J. P. Lu, Q. Si, Ju Kim, and K. Levin (to be published).

[12]S. Doniach, Phys. Rev. B **35**, 1814 (1987).

[13]M. Takigawa and P. C. Hammel (private communication).